CrossMark

Relationship between nano-architectured $Ti_{1-x}Cu_x$ thin film and electrical resistivity for resistance temperature detectors

A. Ferreira[1,*] , J. Borges[1], C. Lopes[1], M. S. Rodrigues[1], S. Lanceros-Mendez[1,2,3], and F. Vaz[1]

[1] Center/Department of Physics, University of Minho, Campus de Gualtar, 4710-057 Braga, Portugal
[2] BCMaterials, Parque Científico y Tecnológico de Bizkaia, 48160 Derio, Spain
[3] IKERBASQUE, Basque Foundation for Science, 48013 Bilbao, Spain

ABSTRACT

$Ti_{1-x}Cu_x$ thin films were produced by the glancing angle deposition technique (GLAD) for resistance temperature measurements. The deposition angle was fixed at $\alpha = 0°$ to growth columnar structures and $\alpha = 45°$ to growth zigzag structures. The Ti-to-Cu atomic concentration was tuned from 0 to 100 at.% of Cu in order to optimize the temperature coefficient of resistance (TCR) value. Increasing the amount of Cu in the $Ti_{1-x}Cu_x$ thin films, the electrical conductivity was gradually changed from 4.35 to $7.87 \times 10^5 \ \Omega^{-1} \ m^{-1}$. After thermal "stabilization," the zigzag structures of $Ti_{1-x}Cu_x$ films induce strong variation of the thermosensitive response of the materials and exhibited a reversible resistivity versus temperature between 35 and 200 °C. The results reveal that the microstructure has an evident influence on the overall response of the films, leading to values of TCR of $8.73 \times 10^{-3} \ °C^{-1}$ for pure copper films and of $4.38 \times 10^{-3} \ °C^{-1}$ for a films of composition $Ti_{0.49}Cu_{0.51}$. These values are very close to the ones reported for the bulk platinum ($3.93 \times 10^{-3} \ °C^{-1}$), which is known to be one of the best material available for these kind of temperature-related applications. The non-existence of hysteresis in the electrical response of consecutive heating and cooling steps indicates the viability of these nanostructured zigzag materials to be used as thermosensitive sensors.

Introduction

Temperature sensors are commonly used in many applications ranging from industrial processes and high vacuum technologies to several examples within the automotive industry [1–3]. The resistance temperature detector (RTD), classified as electrical transducers, is a thermoresistor which can convert temperature variations into electrical resistance variations, acting as a sensor [2]. It has been reported that the standard elements used for RTDs are Platinum (Pt), Nickel (Ni), and Copper (Cu) [4–6]. These pure

Address correspondence to E-mail: armando.f@fisica.uminho.pt

metals are widely used based on their linear response (electrical resistivity vs. temperature), high stability, and reproducibility of the signal in a wide range of temperatures (e.g., −200 to 850 °C for Pt RTD) [5, 6]. While Platinum RTDs are standard temperature sensors, with high linearity, stability, and wide operating range, but are of high cost, Nickel is preferably used in the construction of sensors, with the advantage of being much cheaper. However, nickel and its alloys have high resistivities and high values of temperature coefficient of resistance, but the variation in electrical resistance with temperature is sensitive to strain [5, 6]. In its place, Copper is sometimes used for the range from −100 to 100 °C and is relatively cheap, with high linearity and stability, but practical considerations about the ability to resist to the oxidation limit the choice. Anyway, the relationship between thermo and electrical behavior becomes even more important if the sensing materials are prepared in the form of thin films, since their thermosensitivity can differ significantly from those of the bulk materials in some cases, due to the size effects and (micro/nano)structure [7]. Traditionally, RTDs were wire type, which used film platinum wire covered in insulated tube as the sensing element, but thin film types of RTDs are now replacing the wire type because of their small dimensions and short response time [2, 3, 8]. Combining methods of photolithography and thin film deposition by sputtering offers the possibility of obtaining a hundred sensors on a four inch diameter (Si) wafer with desired resistance variation response [9] offering faster responses when compared to wire-wound counterparts. The construction and characterization of thermal sensors produced by vapor deposition techniques of the Platinum and Titanium (Ti) RTDs have been characterized by Lourenço et al. [8]. The first prototypes show that the platinum deposited on ceramic substrates is highly pure, maintaining the properties of the bulk material and only the density is significantly different, preserving the resistivity, the thermal coefficient of resistance (TCR), and the lattice parameters. Thin film-based technologies permit obtaining smaller and cheaper devices. Traditionally, physical vapor deposition (PVD) technique uses the perpendicular incidence of the particle flux to a typically columnar growth perpendicular to the substrate. The glancing angle deposition, GLAD, method [10], appears to change the typical columnar growth to a designed one-, two- or three-dimensional nanostructures in an uninterrupted process, due to the atomic shadowing effect [11–16]. The idea in creating these structures depends on the materials used in deposition, the incident angle of deposition, and the substrate rotation. The microstructure of the films is strongly dependent on the experimental parameters selected for their fabrication, which affects significantly their response and in-service performance [17–20]. Therefore, a detailed characterization and a careful analysis and correlation of the thin film response with the (micro/nano)structural features are essential.

In this work, Ti–Cu thin films deposited by GLAD were investigated for applications as RTDs. The Ti–Cu system was chosen because it combines the excellent Ti biocompatibility [21–25] with thermal coefficient of resistance of the Cu, offering good thermal, electrical, chemical, and mechanical properties, together with good wear and corrosion resistance. In this particular sense, the present work proposes a non-conventional microstructure (GLAD-like architectures) for measuring temperature variations between 35 and 200 °C through the electrical resistance variations of the $Ti_{1-x}Cu_x$ thin films deposited with different Ti–Cu atomic ratios.

Experimental details

For the current work, thin films with columnar and zigzag-like architectures were studied. A set of $Ti_{1-x}Cu_x$ thin films was deposited onto glass substrates by a home-made DC magnetron sputtering system, using a Ti target positioned at 110 mm from the magnetron (with dimensions $200 \times 100 \times 6$ mm^3 and 99.96 at.% purity). The chamber was pumped down to a base pressure below 4.0×10^{-4} Pa to avoid the presence of oxygen in the films. The target was sputtered with a DC current density of 75 A m^{-2}. The Argon pressure was kept constant at 3.0×10^{-1} Pa for different depositions. The Titanium target was customized with different amounts of Cu pellets in order to change the Copper content in the coatings (with individual area of ~ 0.2 cm^2), symmetrically distributed along the preferential erosion area. All depositions were performed according to the following parameters: 2 zigzag periods, the incident flux angle was fixed at $\alpha = 45°$ and deposition time for zigzag and columnar structures of 2×180 s. For the zigzag thin films, the GLAD sequence was as follows:

1—at a fixed angle ($\alpha = 45°$), growing the layers with a preferred thickness without rotating the substrate holder, 2—rotating the substrate 180° at a faster rotation rate; after that repeat the steps 1 and 2 until the required number of zigzags is obtained. In order to enhance the adhesion of the thin films, the substrates were sputter-cleaned in a plasma reactor (Zepto) for the activation/functionalization of the substrates. The operating conditions of plasma treatments were carried out in a pure Argon atmosphere, during 15 min, after getting a base pressure of about 20 Pa. The power was set to 100 W and the working pressure was approximately 80 Pa.

The morphological features of the $Ti_{1-x}Cu_x$ thin films were probed by Ultra-high-resolution field-emission scanning electron microscope (SEM). Cross-section micrographs were obtained in a FEI Quanta 400FEG ESEM apparatus, operating at 15 keV. Rutherford backscattering spectrometry (RBS) technique was used to measure the atomic composition of the as-deposited samples using a 1.5 or 2 MeV ^{4}He beam, at normal incidence, in a small (RBS) chamber of the IST/LATR 2.5 MeV Van de Graaff accelerator. The composition of the $Ti_{1-x}Cu_x$ samples was obtained using the software NDF, after three different measurements for each sample. The resolution of the atomic concentration of every sample was about 3 at.%.

The thermosensitive response (resistance variation) of the films was also observed in order to evaluate the possibilities of using the films in temperature sensor-based applications. The variation of the electrical resistance of the samples was obtained using an Agilent 34401A multimeter. The temperature was regulated with a Linkam THMSE 600, at a rate of 10 °C min^{-1}, from room temperature to 200 °C. The results were quantitatively analyzed by the Temperature Coefficient of Resistance, α or TCR [26, 27]. The general idea was to analyze the influence of the zigzag nanostructure effect, together with the Cu concentration, on the electrical response of the Ti-based films. The relationship between the measured resistance (R) and the temperature can be expressed as [26]

$$R(T) = R_0\left(1 + AT + BT^2 + CT^3\right), \tag{1}$$

where T represents the temperature in °C; R_0 is the resistance at $T = 0$ °C; and A, B, and C are the Callendar Van Dusen coefficients [26]. The constants A, B, and C, are related with the α and δ coefficients, the first- and second-order temperature coefficient of resistance (TCR), by the following equations.

$$A = \alpha + \frac{\alpha \times \delta}{100}; \quad B = \frac{-\alpha \times \delta}{100^2}; \quad C_{T > 0\,°C} = 0 \tag{2}$$

For $T > 0$ °C, the Eq. (1) can be linearized for small temperature variation ΔT around T. This relation becomes:

$$R(T + \Delta T) = R(T)(1 + \alpha\Delta T), \tag{3}$$

where

$$\alpha = \frac{\Delta R}{R(T)\Delta T}. \tag{4}$$

In Eq. (4), α represents the sensitivity of the RTD sensor in units of °C^{-1}. In order to eliminate misunderstanding, α will be indexed only to incident particle flux hereafter, while TCR will denote the temperature coefficient of resistance.

In order to obtain a stable thermosensitive response, an annealing process was performed after deposition [28]. The experimental protocol for the annealing procedure consisted in the in-air annealing of the films at a constant rate of 10 °C min^{-1}, from room temperature to a maximum temperature of 250 °C. This maximum temperature was then maintained during 6 h, followed by a free cooling stage of the samples, down to room temperature again. At this maximum annealing temperature, the literature review reveals that Ti/Pt thin films suffered a decrease of initial resistance values between 3 and 5% [9], which is claimed to be the result of several structural and microstructural processes, including structural refinement, recrystallization and grain growth, among others [9]. In this work, the TCR and resistivity values were obtained from resistance–temperature calibration curves, measured in two cycles over the range of 35–200 °C.
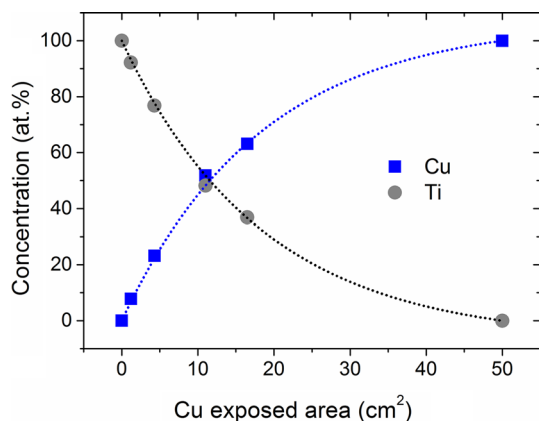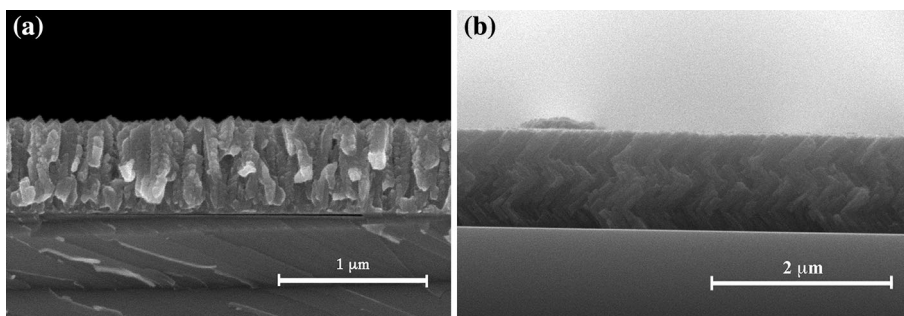
Results and discussion

Chemical composition and electrical conductivity

Figure 1 shows the representative images of the typical columnar (Fig. 1a) and zigzag-type (Fig. 1b) microstructures for Ti films, grown on Si substrates. These images well represent the microstructures of all the samples that are studied in this work.

Thermosensitive tests on the $Ti_{1-x}Cu_x$ thin films, deposited on glass substrates, were prepared with different amounts of Cu in order to optimize the TCR value. The composition of the samples with different

Figure 1 Representative images of the microstructures of the thin films: **a** columnar and **b** 2 zigzag structures for Ti deposited on Si substrates.

Figure 2 Chemical composition as a function of the area of Cu exposed.

Figure 3 Representative images of the microstructures of the thin films: **a** columnar and **b** 2 zigzag structures for Ti deposited on Si substrates.
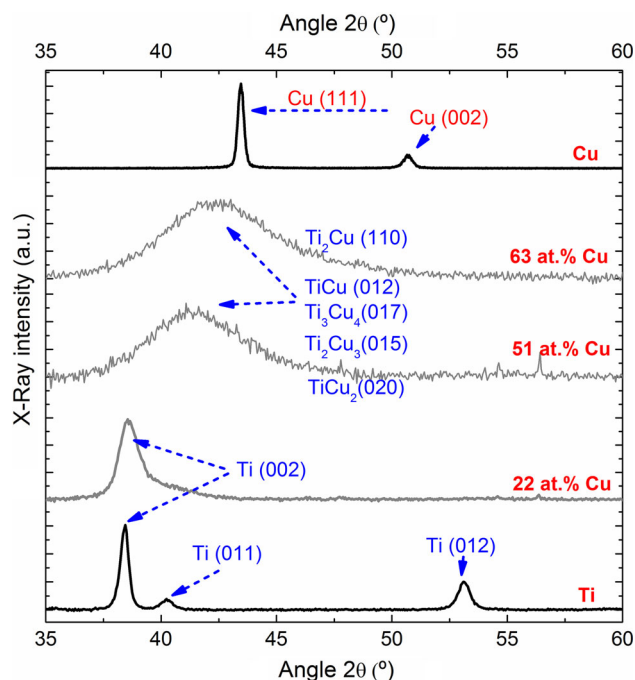
amounts of $Ti_{1-x}Cu_x$ is demonstrated in Fig. 2 as a function of the Cu-exposed area on the Ti target surface. As projected, the results exhibit that the Cu concentration in the films increases with the increasing amount of Cu pellets placed on the surface of the Ti target.

From structural analyses obtained by XRD-diffraction, Fig. 3, the diffraction peaks, characteristic of Ti hexagonal (hcp) structure, with (002), (011), and (012) orientation planes, according to the ICSD collection code: 181,718 suggest a clear evolution from a typical hcp-Ti structure to a fcc-Cu structures, with (111) orientation planes.

In films with Cu content above 50 at.%, it is possible to observe a larger diffraction peak situated at $2\theta \sim 42.5°$, and have several indexing possibilities due to their similar angular positions: Ti_2Cu (110), $TiCu$ (012), Ti_3Cu_4 (017), Ti_2Cu_3 (015), and $TiCu_2$ (020). In this specific diffraction peak, the formation of Ti_3Cu_4 and Ti_2Cu_3 intermetallic phases suggests that they are thermodynamically more favorable [29]. Additionally, for small Cu contents lower to 20 at.%, the films tend to develop a α-Ti(Cu) solid solution structure, where Cu acts as the solute/dopant into

the Ti matrix. Similarly, for atomic content between 50 and 63 at.%, the films tend to grow amorphous Ti–Cu intermetallic, which in fact is in accordance with the Ti–Cu phase diagram for these specific chemical compositions [30]. In the films with atomic content of Cu up to 63.1 at.%, the Ti–Cu intermetallic phases and the possibility of formation of a Cu(Ti) metastable phase cannot be ignored, due to diffraction peak near the Cu (111) orientation.

To evaluate the evolution of the electrical conductivity with incremental Cu content in the films, and to evaluate the possibilities of using the films in RTDs, electrical measurements were performed, Fig. 4.

As expected, the results show that the electrical conductivity increases with the concentration of Cu. Further, the $Ti_{1-x}Cu_x$ films produced with zigzag
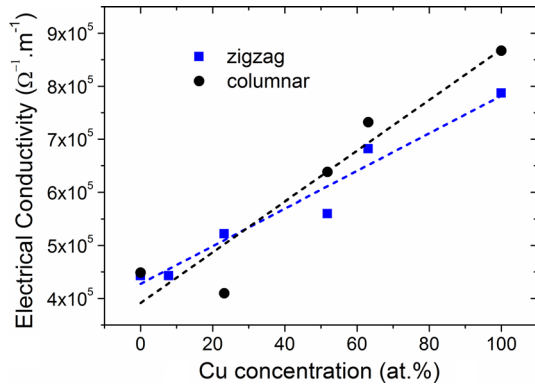
Figure 4 Evolution of the electrical conductivity of the columnar and zigzag structures as a function of the atomic concentration (at.%) of Cu.

microstructures exhibit lower electrical conductivities than the columnar ones. Taking into account the chemical composition of the $Ti_{1-x}Cu_x$ films and zigzag structures, the samples exhibited lower conductivity values $(4.35 \times 10^5 \; \Omega^{-1} \, m^{-1})$ for small

concentrations of Cu (<10 at.%) and the electrical conductivity increases up to $7.87 \times 10^5 \; \Omega^{-1} \, m^{-1}$ for the pure Cu film. The high disordered structure of the zigzag films, mainly composed by the amorphous metastable α-Ti(Cu) phase, increases the number of structural defects, and hence the number of "scattering traps" for the charge carriers, resulting in higher electrical resistivity values, when compared with crystalline materials [15]. For these specific chemical compositions, the particular nature of the intermetallic phases revealed to be particularly important for the $Ti_{1-x}Cu_x$ electrical response as it will be further confirmed later is this work for the thin films under analysis.

Thermosensitive response

Figure 5 shows representative measurements of the thermosensitive response (resistance variation) of the films with temperature applied to all samples.
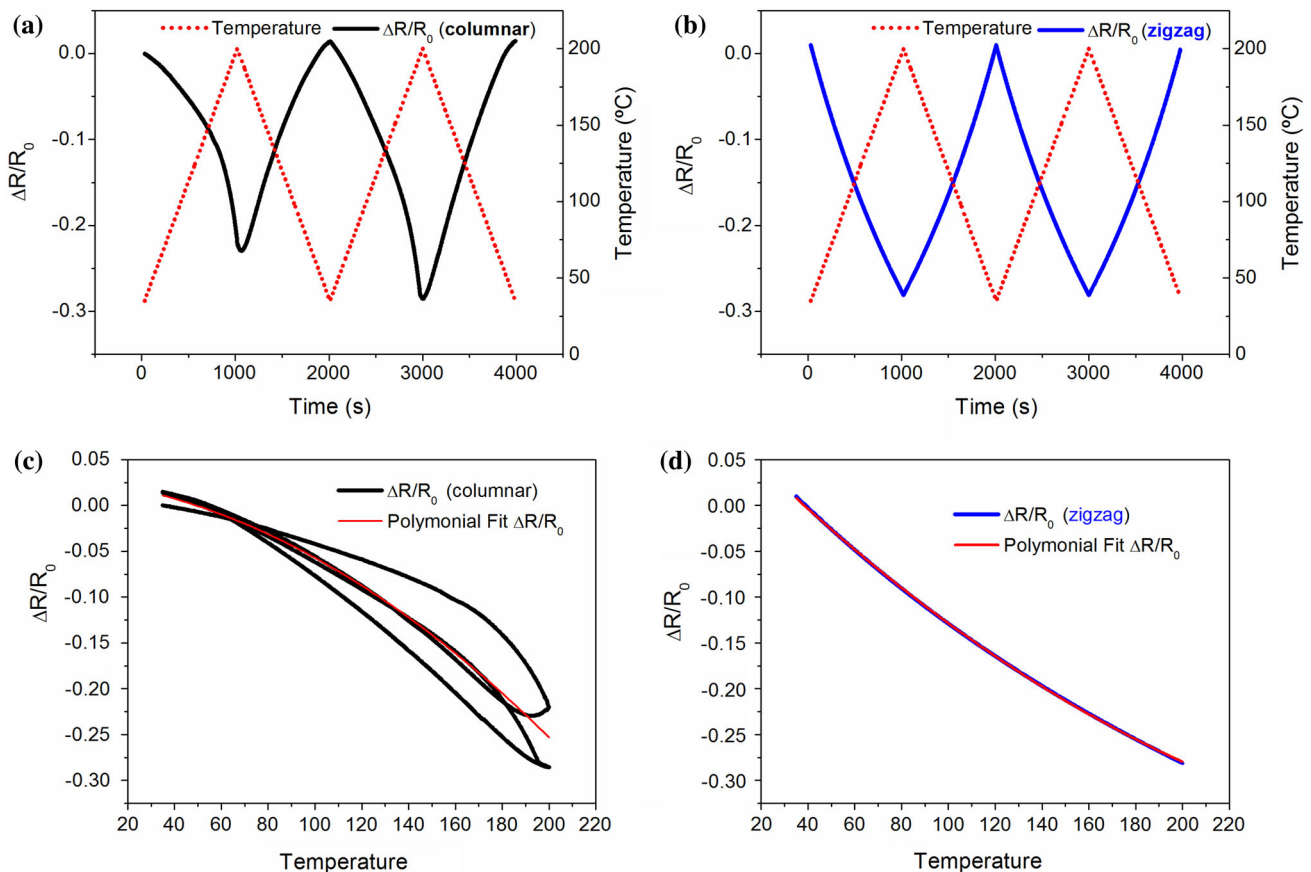
Figure 5 Thermosensitive response of $Ti_{0.49}Cu_{0.51}$ films deposited on glass substrates with, **a** conventional columnar growth, **b** zigzag-like architecture (2 zigzag periods); and $\Delta R/R$ variation as a function of temperature for the, **c** columnar-like thin films and **d** zigzag-like thin films.

Table 1 Values of TCR for the $Ti_{1-x}Cu_x$ films deposited on glass substrates

	Columnar TCR ($\times 10^{-3}$ °C^{-1})	Zigzag TCR ($\times 10^{-3}$ °C^{-1})
Ti	0.26 ± 0.02	1.96 ± 0.03
$Ti_{0.77}Cu_{0.23}$	0.30 ± 0.03	2.58 ± 0.01
$Ti_{0.49}Cu_{0.51}$	1.92 ± 0.04	4.59 ± 0.02
$Ti_{0.37}Cu_{0.63}$	0.22 ± 0.01	7.88 ± 0.03
Cu	–	9.57 ± 0.08

Regarding the thin film structure under study in this work, the experimental results show that when the $Ti_{1-x}Cu_x$ thin films are subjected to a temperature variation, with in situ electrical resistance measurements, a sharp decrease of the initial electrical resistance is observed for temperatures between 35 and 200 °C. This behavior is representative for the different heating and cooling cycles, as well as for the different samples, as shown in Fig. 5a and b.

The analysis of Fig. 5, reveals that the $Ti_{1-x}Cu_x$ thin films, produced with a zigzag microstructure (Fig. 5b), do not exhibit changes in the initial resistivity after consecutive heating steps, which is significantly different when compared to that of columnar thin films (Fig. 5a). At the same time, the $\Delta R/R$ slope variation as a function of temperature for the $Ti_{0,49}Cu_{0,51}$ columnar thin film (Fig. 5c), shows significant hysteresis in the electrical response as a result of the consecutive heating and cooling cycles. However, this hysteresis behavior is eliminated when the same film is made in with a zigzag structure (Fig. 5d), suggesting the relevance of the nanostructure on the electrical resistivity response. According to Zhang et al. [31], the resistivity is not influenced by consecutive annealing steps, which is in agreement with the results obtained when the film was produced in a zigzag microstructure. After thermal "stabilization" of the $Ti_{1-x}Cu_x$ films, by performing annealing at 250 °C for 6 h, the phenomenon grain boundary oxidation gives rise to negative TCR values in thin metallic film, Fig. 5c and d [32]. Peripheral parts of the zigzag columns are initially oxidized and the film microstructure can be assumed as a heterogeneous multiphase (metal–insulator) system, which is electrically discontinuous. The internal zone of the columns acts as an electron-conductive phase (metallic part) bordered by sub-stoichiometric oxide compounds (isolating shell). The intercolumnar distance resulting from the deposition at an incident

angle of 45°, combined with the oxide layer of the peripheral parts of the zigzag columns, which gradually thickens with the rising of the temperature, are both acting as potential barriers, leading to negative TRC values [32].

Using Eq. (4), one can obtain the linear constant of the polynomial fit in Fig. 5c and d, which corresponds to the temperature coefficient of resistance, TCR. The obtained values are summarized in Table 1.

The final value for $Ti_{0.49}Cu_{0.51}$ (Table 1) is very close to the values reported for bulk Pt (3.93×10^{-3} °C^{-1}) [31], increasing for Cu amounts above 0.51 at.%, where the amorphous Ti–Cu intermetallic phases appear. Therefore, the values of the TCR obtained above (Table 1) show a strong intrinsic contribution of the Cu to the sensitivity of the films for a Cu concentration above 23.2 at.% and zigzag structures, as observed by comparison with the value of columnar TCR. However, for $Ti_{1-x}Cu_x$ thin films produced with Cu amounts below 0.51 at.%, the TCR values were even slightly lower than the reference Pt RTDs. In the case of columnar thin films, the lower TCR values, at the moment, can only be attributed to the specific nanostructure that was developed. In fact, all films, columnar and zigzag architectured, were in-air annealed using the same procedure. Thus, it is also possible that some micro(structural) defects resulted from the deposition itself. Processes such as self-diffusion, recrystallization, grain growth, and annealing may affect the stability of the columnar film, which are, somehow, not observed or attenuated in the films produced with zigzag structures due to its particular nanostructure (spring effect).

The values of the TCR and the non-existence of hysteresis in the electrical response of consecutive annealing steps, over a wide range of temperatures, indicate the viability of these nanostructured zigzag materials to be used as thermosensitive sensors.

Conclusion

$Ti_{1-x}Cu_x$ thin films were sputter deposited by systematically varying the concentrations of copper, to be applied as thermosensitive thin films. Upon increasing the amount of Cu in the $Ti_{1-x}Cu_x$ thin films, the change in electrical conductivity of the films induces strong variation of the thermosensitive response of the materials. The results show that the microstructure developed in the films has a

pronounced influence on the overall sensor response leading to maximum TCR values of 9.57×10^{-3} °C^{-1} for the pure copper sample with a zigzag structure.

References

[1] Hughes TA (2007) Measurement and Control Basics. ISA

[2] Chung G-S, Kim C-H (2008) RTD characteristics for micro-thermal sensors. Microelectron J 39(12):1560–1563. doi:10.1016/j.mejo.2008.02.028

[3] Kim J, Kim J, Shin Y, Yoon Y (2001) A study on the fabrication of an RTD (resistance temperature detector) by using Pt thin film. Korean J Chem Eng 18(1):61–66

[4] Sen SK, Pan TK, Ghosal P (2011) An improved lead wire compensation technique for conventional four wire resistance temperature detectors (RTDs). Measurement 44(5):842–846. doi:10.1016/j.measurement.2011.01.019

[5] Borges J, Martin N, Barradas NP, Alves E, Eyidi D, Beaufort MF, Riviere JP, Vaz F, Marques L (2012) Electrical properties of AlNxOy thin films prepared by reactive magnetron sputtering. Thin Solid Films 520(21):6709–6717. doi:10.1016/j.tsf.2012.06.062

[6] Childs PRN, Greenwood JR, Long CA (2000) Review of temperature measurement. Rev Sci Instrum 71(8):2959–2978. doi:10.1063/1.1305516

[7] Lu N, Wang X, Suo Z, Vlassak J (2009) Failure by simultaneous grain growth, strain localization, and interface debonding in metal films on polymer substrates. J Mater Res 24(02):379–385. doi:10.1557/JMR.2009.0048

[8] Lourenço MJ, Serra JM, Nunes MR, Vallêra AM, de Castro CAN (1998) Thin-film characterization for high-temperature applications. Int J Thermophys 19(4):1253–1265. doi:10.1023/a:1022614431285

[9] Zribi A, Barthès M, Bégot S, Lanzetta F, Rauch JY, Moutarlier V (2016) Design, fabrication and characterization of thin film resistances for heat flux sensing application. Sens Actuators, A 245:26–39. doi:10.1016/j.sna.2016.04.040

[10] Knorr TG, Hoffman RW (1959) Dependence of geometric magnetic anisotropy in thin iron films. Phys Rev 113(4):1039–1046

[11] Ferreira A, Borges J, Lopes C, Martin N, Lanceros-Mendez S, Vaz F (2016) Piezoresistive response of nano-architectured Ti$_x$Cu$_y$ thin films for sensor applications. Sens Actuators, A 247:105–114. doi:10.1016/j.sna.2016.05.033

[12] Ferreira A, Lopes C, Martin N, Lanceros-Méndez S, Vaz F (2014) Nanostructured functional Ti–Ag electrodes for large deformation sensor applications. Sens Actuators A 220:204–212. doi:10.1016/j.sna.2014.09.031

[13] Besnard A, Martin N, Carpentier L, Gallas B (2011) A theoretical model for the electrical properties of chromium thin films sputter deposited at oblique incidence. J Phys D Appl Phys 44(21):215301

[14] Besnard A, Carpentier L, Martin N, Rauch J-Y (2013) Metal-to-dielectric transition induced by annealing of oriented titanium thin films. Funct Mater Lett 06(01):1250051. doi:10.1142/S1793604712500518

[15] Lopes C, Vieira M, Borges J, Fernandes J, Rodrigues MS, Alves E, Barradas NP, Apreutesei M, Steyer P, Tavares CJ, Cunha L, Vaz F (2015) Multifunctional Ti–Me (Me=Al, Cu) thin film systems for biomedical sensing devices. Vacuum, Part B 122:353–359. doi:10.1016/j.vacuum.2015.05.015

[16] Lopes C, Pedrosa P, Martin N, Barradas NP, Alves E, Vaz F (2015) Study of the electrical behavior of nanostructured Ti–Ag thin films, prepared by glancing angle deposition. Mater Lett 157:188–192. doi:10.1016/j.matlet.2015.05.067

[17] Thornton JA (1986) The microstructure of sputter-deposited coatings. J Vac Sci Technol 4(6):3059. doi:10.1116/1.573628

[18] Messier R (1984) Revised structure zone model for thin film physical structure. J Vac Sci Technol 2(2):500. doi:10.1116/1.572604

[19] Petrov I, Barna PB, Hultman L, Greene JE (2003) Microstructural evolution during film growth. J Vac Sci Technol A 21(5):S117. doi:10.1116/1.1601610

[20] Mahieu S, Ghekiere P, Depla D, De Gryse R (2006) Biaxial alignment in sputter deposited thin films. Thin Solid Films 515(4):1229–1249. doi:10.1016/j.tsf.2006.06.027

[21] Lopes C, Gonçalves C, Pedrosa P, Macedo F, Alves E, Barradas NP, Martin N, Fonseca C, Vaz F (2013) TiAgx thin films for lower limb prosthesis pressure sensors: Effect of composition and structural changes on the electrical and thermal response of the films. Appl Surf Sci Part A 285:10–18. doi:10.1016/j.apsusc.2013.07.021

[22] Gonçalves C, Lopes C, Fonseca C, Guedes A, Vaz F (2013) Structural and morphological evolution in TiAgx thin films as a function of in-vacuum thermal annealing J Nano Res 25:67–76. 10.4028/http://www.scientific.net/JNanoR.25.67

[23] Ewald A, Gluckermann SK, Thull R, Gbureck U (2006) Antimicrobial titanium/silver PVD coatings on titanium. Biomed Eng Online 5:1–10. doi:10.1186/1475-925X-5-22

[24] Takahashi M, Kikuchi M, Takada Y, Okuno O (2005) Grindability and mechanical properties of experimental Ti–Au, Ti–Ag and Ti–Cu alloys. Int Congr Ser 1284:326–327. doi:10.1016/j.ics.2005.06.006

[25] Kikuchi M, Takahashi M, Okuno O (2008) Machinability of experimental Ti–Ag alloys. Dent Mater J 27(2):216–220

[26] Dusen MSV (1925) Platinun-resistance thermometry at low temperatures. J Am Chem Soc 47(2):326–332. doi:10.1021/ja01679a007

[27] Sinclair DC, West AR (1989) Impedance and modulus spectroscopy of semiconducting BaTiO$_3$ showing positive temperature coefficient of resistance. J Appl Phys 66(8):3850–3856. doi:10.1063/1.344049

[28] Lopes C, Gonçalves C, Borges J, Polcar T, Rodrigues MS, Barradas NP, Alves E, Le Bourhis E, Couto FM, Macedo F, Fonseca C, Vaz F (2015) Evolution of the functional properties of titanium-silver thin films for biomedical applications: Influence of in-vacuum annealing. Surf Coat Technol 261:262–271. doi:10.1016/j.surfcoat.2014.11.020

[29] Gupta KP (2002) The Cu–Ni–Ti (Copper–Nickel–Titanium) system. J Phase Equilibria 23(6):541. doi:10.1361/105497102770331299

[30] Murray JL (1983) The Cu–Ti (Copper–Titanium) system. Bull Alloy Phase Diagr 4(1):81–95. doi:10.1007/bf02880329

[31] Jialiang Z, Yoshimichi N, Saburo K, Yoshinori I (1997) Microstructure and temperature coefficient of resistance of platinum films. Jpn J Appl Phys 36(2R):834

[32] Chopra KL, Pandya DK (1978) Thin film thermal device applications. Thin Solid Films 50:81–98. doi:10.1016/0040-6090(78)90095-0